J. Appl. Comput. Mech., 5(2) (2019) 181-191
DOI: 10.22055/JACM.2018.25311.1243

ISSN: 2383-4536
jacm.scu.ac.ir

M&MoCS

Shahid Chamran University of Ahvaz

Journal of Applied and Computational Mechanics

Research Paper

Numerical Investigation of the Effect of Bubble-Bubble Interaction on the Power of Propagated Pressure Waves

M. Khojasteh-Manesh, M. Mahdi

Department of Mechanical Engineering, Shahid Rajaee Teacher Training University, Tehran, Iran

Received March 18 2018; Revised May 19 2018; Accepted for publication June 28 2018.
Corresponding author: Miralam Mahdi, M.Mahdi@sru.ac.ir

Abstract. The study of bubble dynamics, especially the interaction of bubbles, has drawn considerable attention due to its various applications in engineering and science. Meanwhile, the study of the oscillation effect of a bubble on the emitted pressure wave of another bubble in an acoustic field has less been investigated. This issue is investigated in the present study using the coupling of Keller-Miksis and Gilmore models. The ordinary differential equations are solved using MATLAB software and Runge-Kutta forth order method with the adaptive step size control. The results show the dependence of bubbles behavior and the strength of their pressure waves on two parameters of the initial radius and the bubbles center-to-center distance. As the initial radius of the adjacent bubble grows, its effect on the other bubble increases and causes a reduction in the other bubble maximum radius, wall velocity, internal pressure, and emitted pressure wave intensity. However, increasing the initial distance of the bubbles reduces the effect of the bubbles on each other and causes their behaviors become closer to the single-bubble oscillation mode.

Keywords: Bubble dynamics; Nonlinear oscillation; Mutual interaction; Pressure wave; Shock wave.

1. Introduction

The nonlinear behavior of a cavitation bubble in an oscillating pressure field is a complicated phenomenon which its understanding has greatly contributed to the various technological advancements since the past century. This phenomenon is usually associated with a sharp rise in the internal pressure, temperature, wall velocity, and wall acceleration of the bubble [1,2]. Sonoluminescence or light emission from the bubble is also a probable consequence of the bubble collapse which has been studied by many researchers [3–7]. The microjet formation and the shock wave radiation are two other important results of the bubbles violent collapse [8]. The pressure waves (shock waves), which are the results of the strong compression of the bubble content at its minimum volume, are created in the volume increment period after the bubble collapse. The magnitudes of these pressure waves might reach the order of GPa [9] and they can cause an extreme damage to the ship propeller or pump impeller blades [10].

In addition to the single-bubble case, the study of interactions and factors affecting the behavior of bubbles in multi-bubble systems is also a significant issue in the field of bubble dynamics [11]. As it is proven in various articles, the effect of bubbles on each other can lead to different results. For example, the collapse of a bubble can strengthen or weaken the collapse of the other bubble, affect its collapsing time, cause the given bubble to be attracted or repelled, etc. [12–15].

Despite the existence of numerous experimental works [16–18] and due to some limitations, such as rapid changes in properties in order of milliseconds [16] and high temperatures and pressures during collapse period [6,19], the empirical methods have encountered difficulties. These limitations have intensified the significance of numerical works as methods with a less amount of risk and a wider scope of activity. A concise summary of a number of studies on bubble dynamics is presented in the following section.

Theoretical studies on the bubble dynamics are based on the fundamental works of Lord Rayleigh [20], who proposed the

Published online: January 17 2019

Rayleigh equations for the pressure prediction during the collapse of a spherical bubble. Since then, the bubble oscillation equations and models have been developed and modified under various assumptions [21–23]. Using these equations, Fuster et al. [24] studied the effect of liquid compressibility on the behavior of a single spherical bubble, considering mass, momentum, and energy equations. They found that for intense collapses in which pressures at the bubble interface exceed 1000 atm, the liquid compressibility should be taken into account for the accurate prediction of bubble dynamics. Minsier and Proost [25] numerically modeled the shock waves emitted during the spherical bubble collapse and found that these waves are strong enough to delaminate typical device structures. Mahdi et al. [26] studied the collapse of spherical bubble by taking into account the heat transfer effects and concluded that the emitted shock waves strength is related to the acoustic field amplitude and the initial bubble radius. Shaw and Spelt [27] numerically investigated the bubble collapse shock waves and implied that there is a linear relationship between the maximum radius of the bubble and both strength and width of the shock waves. Studying the behavior of a sonoluminescing gas bubble, Karng et al. [28] measured the shock pulse emitting from a single sonoluminescing gas bubble with a needle hydrophone and compared it with the simulated results. They reported that the bubble wall velocity and the wall pressure near the collapse could dramatically affect these values.

In the mutual interaction case, Crum [12] measured the translational force between two bubbles and concluded that the amount of this force is negligible compared to the primary Bjerknes and buoyant forces. Mettin et al. [14] investigated the secondary Bjerknes forces between two interacting bubbles in a strong acoustic field. They showed that in cases where the equilibrium bubble radius is a little larger than the dynamical Blake threshold, the interaction force could be changed from attraction to repulsion. Ida [29] studied the mutual interaction of bubbles through pressure pulses and found that the instantaneous radius and the internal pressure of bubbles can affect the amplitude of negative reflected pulses. Sadighi-Bonabi et al. [30] numerically investigated the mutual interaction of two oscillating gas bubbles in different concentrations of sulfuric acid and found that the acid viscosity can change both the sign and the value of the secondary Bjerknes force. Li et al. [31] studied the behavior of two bubbles in the hydrodynamic cavitation and noticed the changes in the bubbles oscillation time, the radius growth, and the pressure pulse compared to the single-bubble state.

As mentioned above, although several researchers have investigated pressure waves and mutual interaction of bubbles in an acoustic field, the effects of bubbles interaction on their emitted pressure waves has not been extensively investigated.

In the present study, as a confirmation of the accuracy of the numerical results, initially a comparison was carried out between the empirical and numerical values of the bubble radius. The same process was applied on the empirical and numerical values of the simulated pressure wave. Then, each two bubbles with a fixed center-to-center distance were selected and their initial radius effects on the behavior of bubbles were shown. After that, the initial radii of the bubbles were considered as constant and the effect of the distance change was investigated. For both modes, diagrams of the variation of pressure wave power were depicted and the causes of its changes was investigated.

2. Mathematical Model

2.1 Calculating bubble dynamics

In order to explain the radial oscillation of a spherical bubble in a compressible liquid, the Keller-Miksis equation is used:

$$\left(1-\frac{\dot{R}}{c}\right)R\ddot{R}+\left(\frac{3}{2}-\frac{\dot{R}}{2c}\right)\dot{R}^2=\frac{1}{\rho}\left(1+\frac{\dot{R}}{c}\right)\left[P_w-P_0-P_{ex}\right]+\frac{R}{\rho c}\frac{\mathrm{d}}{\mathrm{d}t}\left[P_w-P_{ex}\right] \tag{1}$$

$$P_w=P_b-\frac{2\sigma}{R}-\frac{4\mu}{R}\dot{R} \tag{2}$$

$$P_b=\left(P_0+\frac{2\sigma}{R_0}\right)\left(\frac{R_0^3-h^3}{R^3-h^3}\right)^{\kappa} \tag{3}$$

where c is the speed of sound in the liquid, R is the instantaneous radius of the bubble varying with time t, and $\dot{R}$ and $\ddot{R}$ represent the first and second derivatives of R, respectively. ρ is the liquid density and P_w describes the liquid pressure at the bubble wall. P_0 and P_{ex} are the atmospheric pressure and the exerted driving pressure, respectively. P_b is the pressure inside the bubble and assumed as uniform. σ and μ denote the surface tension and the liquid viscosity, respectively. R_0 represents the equilibrium radius, h stands for the hard-core Van der Waals radius, and κ is the polytropic exponent.

The Keller-Miksis equation in its basic form is suitable for detecting the behavior of a single spherical bubble. In case of multi-bubble, it is necessary to consider some modifications in this equation. Because if the center-to-center distance between bubbles are small enough, the pressure wave radiated by the neighboring bubbles is no longer negligible and should be taken into account. In fact, the presence of the neighboring bubble causes the pressure field to be changed around the first bubble. As a result of this change, the driving pressure is no longer equal to the external driving pressure. In other words, in multi-bubbles case, the pressure wave emitted from the neighboring bubble combines with the external driving pressure and affects the behavior of the first bubble as a new driving pressure [29].

Using Euler and continuity equations, one can obtain the amplitude of the pressure wave radiated by a spherical bubble undergoing volume change,

$$\frac{\partial u}{\partial t}+u\frac{\partial u}{\partial r}=-\frac{1}{\rho}\frac{\partial p}{\partial r} \tag{4}$$

$$\frac{\partial r^2 u}{\partial r}=0 \tag{5}$$

where $u(r,t)$ and $p(r,t)$ represent the velocity and the pressure in the liquid, respectively, and r is the distance from center of the bubble. Integrating Eq. (5) with respect to r and assuming $u(R,t)=\dot{R}(t)$ and $u(r\to\infty,t)=0$, gives

$$u=\frac{R^2}{r^2}\dot{R} \tag{6}$$

Substituting Eq. (6) into Eq. (4) and assuming $p(r\to\infty,t)=0$ and integrating it, yields

$$p=\frac{\rho}{r}\frac{d(R^2\dot{R})}{dt}+O(\frac{1}{r^4}) \tag{7}$$

This pressure is the pressure wave emitted from each of the bubbles. Therefore, subscripts *i* and *j* are used to show the individual effect of each bubble (*i* for the first bubble and *j* for the second bubble). Adding this pressure to the external driving pressure yields

$$p_{ex\,(\text{new})}(t)=p_{ex}(t)+\sum_{j=1,j\neq i}^{2}p_j \tag{8}$$

Substituting Eq. (8) into Eq. (1) and neglecting the terms in the order of $(R_j/D_{i,j})(\dot{R}_i/c)$ and $(R_i/D_{i,j})[d^2(\dot{R}_j/c)/dt^2]$, one can obtain the modified Keller-Miksis equation for bubble *i* [14] as

$$\left(1-\frac{\dot{R}_i}{c}\right)R_i\ddot{R}_i+\left(\frac{3}{2}-\frac{\dot{R}_i}{2c}\right)\dot{R}_i^2=\frac{1}{\rho}\left(1+\frac{\dot{R}_i}{c}\right)\left[P_{w,i}-P_0-P_{ex}\right]+\frac{R_i}{\rho c}\frac{\mathrm{d}}{\mathrm{d}t}\left[P_{w,i}-P_{ex}\right]-\sum_{j=1,j\neq i}^{2}\frac{1}{D_{i,j}}\frac{\mathrm{d}\left(R_j^2\dot{R}_j\right)}{\mathrm{d}t} \tag{9}$$

$$P_{w,i}=P_{b,i}-\frac{2\sigma}{R_i}-\frac{4\mu}{R_i}\dot{R}_i \tag{10}$$

$$P_{b,i}=\left(P_0+\frac{2\sigma}{R_{0,i}}\right)\left(\frac{R_{0,i}^3-h_i^3}{R_i^3-h_i^3}\right)^{\kappa} \tag{11}$$

where $D_{i,j}$ in Eq. (9) is the distance between bubbles centers. Here, the gas inside bubbles is assumed to be a Van der Waals gas and the polytropic exponent of the gas κ is assumed to be equal to its specific heat ratio γ which means that the compression process is considered to be adiabatic. The vapor pressure and the mass exchange between the bubble and the liquid are neglected for simplicity.

2.2. Calculating emitted pressure wave

In deriving the distributed pressure field in the liquid, the method presented by Gilmore [21] (which is based on Kirkwood-Bethe assumption) is applied. For evaluating the pressure field, it is necessary to determine the characteristic curve and the velocity field.

$$y_i=\frac{R_i\dot{R}_i^2}{2}+\frac{R_i\left(P_{b,i}-P_\infty\right)}{\rho}\left(1-\frac{P_{b,i}-P_\infty}{2\rho c^2}\right)-\frac{2\sigma}{\rho}-\frac{4\mu\dot{R}_i}{\rho} \tag{12}$$

$$u_i(r,t)=\frac{y_i}{cr_i}+\frac{K_i y_i^2}{c^3 r_i^2}\left(1-\frac{y_i}{c^2 r_i}+\frac{K_i^2 y_i^4}{2c^8 r_i^4}\right) \tag{13}$$

$$K_i=\frac{c^3 R_i^2\dot{R}_i}{y^2}\left(1-\frac{\dot{R}_i^2}{2c^2}\right)-\frac{c^2 R_i}{y_i}\left(1-\frac{\dot{R}_i}{c}\right) \tag{14}$$

$$t_i=t_{R_i}+\left(\frac{r_i-R_i}{c}\right)\left(1-\frac{\dot{R}_i R_i}{cr_i}\right) \tag{15}$$

In the above-mentioned equations, y_i is the characteristic curve and u_i is the velocity field in the liquid due to the collapse of bubble *i*. r_i is the distance from the bubble center and is different from $D_{i,j}$. $P_\infty=P_0+P_{ex}$ is the ambient pressure and

t_{R_i} is the time at which the radius of the bubble is R_i. In other words, it takes a finite time $t - t_R$ for an event which happens in the bubbles wall at the instant of t_R to reach to the point r in the liquid. When the characteristic curve and the velocity field are calculated, the pressure field can be determined as follows:

$$p_i(r,t) = P_\infty + \rho\left(\frac{y_i}{r_i} - \frac{u_i^2}{2}\right) + \frac{\rho}{2c^2}\left(\frac{y_i}{r_i} - \frac{u_i^2}{2}\right)^2 \tag{16}$$

The above-mentioned equations (1-16) are written for the first bubble. By replacing the indices *i* and *j*, these equations are obtained for the second bubble. The set of these equations is then solved simultaneously using MATLAB software and the Runge-Kutta forth order method with an adaptive time step.

3. Results and discussion

3.1. Validation of numerical model

First, to ensure the accuracy of the results in predicting the behavior of the bubble, the simulated bubble behavior result is compared with the experimental data reported by Flannigan et al. [32]. Figure 1 shows the variation of the radius of the argon gas bubble ($k = 1.67$) with the initial radius of $R_0 = 13$ μm in sulfuric acid with $\mu = 0.02036$ kg/m.s, $\sigma = 0.055$ N/m, and $\rho = 1714$ kg/ m^3. This bubble is under the sinusoidal stimulation wave of $P_{ex} = -P_a \sin(2\pi ft)$ with the amplitude $P_a = 1.42P_0$, the initial pressure $P_0 = 1$ atm, and the frequency $f = 28.5$ kHz. As can be seen, there is a good agreement between the numerical solution and the empirical values at the growth stage, the collapse, and the first rebound of the bubble. However, in next rebounds, the experimental data shows greater dampening than that predicted by simulations. This could be due to other factors that can influence the bubble behavior which have not been considered in our simulations. Those factors may include the effect of chemical reactions as well as the effect of mass and heat transfer at the bubble wall [1].

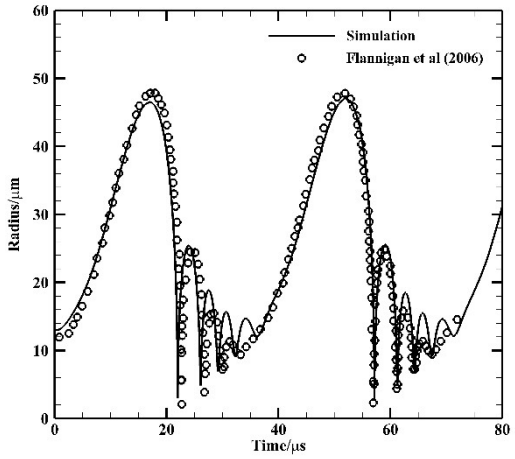

Fig. 1. Dynamic behavior of the argon bubble in sulfuric acid

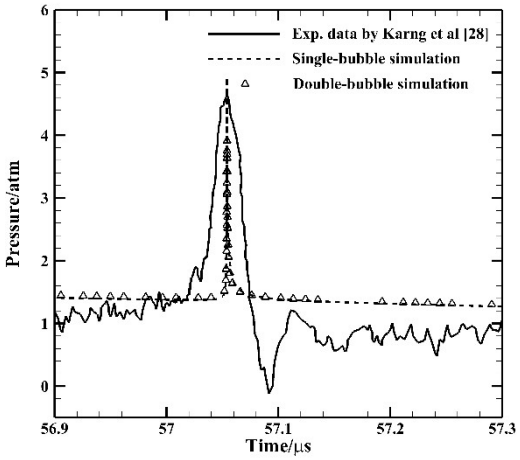

Fig. 2. Measured and simulated pressure waves at the distance of 3mm from center of the 4.5-μm bubble in single-bubble and double-bubble cases

In Fig. 2, a comparison is made between measured values of the propagated pressure wave by Karng et al. [28] and simulated values in single-bubble and double-bubble modes. Since there is no experimental data for comparing pressure waves in single-bubble and double-bubble cases, the experimental data for the single-bubble case are used for validation. Here, the initial radius of the bubble is $R_0 = 4.5$ μm. The driving pressure is assumed to be $P_{ex} = -P_a \sin(2\pi ft)$ in which $P_a = 1.35\,P_0$, $P_0 = 1$ atm, and $f = 28.9$ kHz. The fluids are air with $k = 1.4$ and $h = R_0 / 8.54$ for the gas inside the bubble and water with $\mu = 0.0010016$ kg/m.s, $\sigma = 0.07275$ N/m, $\rho = 998$ kg/ m^3, and $c = 1500$ m/s as the surrounding liquid. For the double-bubble case, a bubble with the initial radius of $R_0 = 12$ μm is placed at 200 μm distance from the first bubble. As can be seen, the maximum measured value of the pressure wave in the single-bubble case is about 4.6 atm which is overestimated about 6 percent by the numerical simulation. It is also noticeable that in double-bubble case, where 4.5-μm and 12-μm bubbles are coupled to each other, the magnitude of the pressure wave reduced to about 3.9 atm. This change is due to the existence of the 12-μm bubble. In other words, the radial motion of the smaller bubble is suppressed by the bigger one. All over, despite the existence of a slight overestimation, it can be said that the accuracy of numerical simulation is still acceptable.

3.2. Numerical results

After ensuring the accuracy of results in single-bubble case, the mutual interaction of bubbles is investigated. For this purpose, three bubbles with initial radii of $R_0 = 12, 8$ and 4 μm are placed in pair under the stimulation wave of $P_{ex} = -P_a \sin(2\pi ft)$ with $P_a = 1.2\,P_0$, $P_0 = 1$ atm, and $f = 12$ kHz. The fluids in this simulation are also air and water with the same above-mentioned specifications.

3.2.1. Effect of bubbles initial radius

In order to investigate the effect of initial radius on the behavior of bubbles, at first, the distance between two bubbles is considered to be fixed and the effect of the radius parameter is investigated. It is important to note that since the two bubbles are assumed spherical, the distance between them should be determined in a way that interference of the bubbles be prevented [14]. For this purpose, the distance between bubbles is initially assumed to be 200 μm and then 500 μm, which both are more than the sum of the maximum values of their radii before the collapse. Figure 3 shows the schematic of two bubbles examined in the present study.

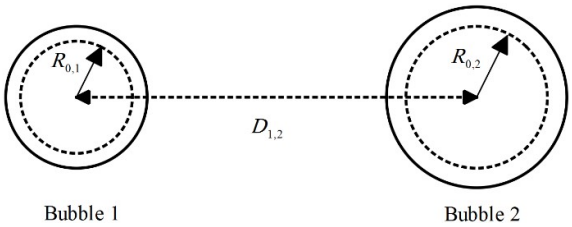

Fig. 3. Schematic of two oscillating bubbles

Figure 4 shows the behavior of the bubble with the initial radius of $R_0 = 8$ μm in the presence of bubbles with the initial size of $R_0 = 4$, 8, and 12 μm at the distance of $D = 200$ μm from the intended bubble. For a better comparison, the behavior of this bubble is also given in the absence of the other bubbles (the state $D \to \infty$). As already mentioned, the interaction of bubbles with each other is accomplished through the propagation of pressure waves, followed by a change in the pressure field around the bubbles. Therefore, according to Fig. 4, it can be noticed that the changes in the pressure field around the first bubble depends on the radius of the neighboring bubble. As can be seen in Fig. 4(a), the highest growth of the bubble radius is related to the single-bubble mode. By placing the smaller bubble in the vicinity of the given bubble, the maximum magnitude of the graph is slightly decreased. As the initial radius of the adjacent bubble increases, its effect on the desired bubble is also increased. For example, by placing the bubble with the initial radius of R_0 =8 μm in the vicinity of the desired bubble, the maximum radius is decreased by about 6 percent and by placing the bubble with the initial radius of R_0 =12 μm, the maximum radius is reduced by about 10 percent. It is also noticeable that the presence of the second bubble causes a lag in the oscillation of the 8-μm bubble. Although this lag is due to the existence of interaction term on the right-hand-side of Eq. (9), there is no explicit relationship between the amount of lag and radius of the second bubble.

Figure 4(b) shows the wall velocity of the bubble. As is shown, in comparison with the single-bubble state, by placing an equal size or a larger size bubble in the vicinity of the 8-μm bubble, the magnitude of the wall velocity is decreased. For example, by placing a12-μm bubble next to a 8-μm one, the smaller bubble wall velocity reduces about 28 percent. However, by placing a smaller bubble next to the given one, the wall velocity does not change significantly. It is also noticeable that the maximum value of wall velocity (at the stage of volume increment after the collapse) is approximately equal in all four modes. Figure 4(c) shows the internal pressure of the 8-μm bubble in different situations which is valid for all points within the bubble. In comparison with the single-bubble case, by placing an equal bubble next to the 8-μm bubble, the maximum internal pressure reduces about 9 percent and by replacing it with a greater bubble, the reduction changes up to 40 percent. Figures 4(d) and 4(e) illustrate the propagated shock waves of a 8-μm bubble. In Fig. 4(d), the shock waves are shown for both single-bubble case and the case where the 4-μm bubble is located at the distance of 200 μm from the bubble center. In Fig. 4(e), the shock waves

are shown for the cases in which the bubbles with initial radii of R_0 =12 μm and R_0 =8 μm are situated at the distance of 200 μm. These waves are depicted at $r = 200$ μm and $r = 500$ μm from the bubble center. As it shows, although the shock strength of the 8-μm bubble is not significantly changed in the presence of the smaller bubble (about 1.5 percent decrease in Fig. 4(d)), it is remarkably affected by the presence of the equal and larger size bubbles. For example, at the distance of $r = 200$ μm from the bubble center, the shock wave power in 8-8 mode and 8-12 mode is about 6 percent and 21 percent lower than the value of the single-bubble case, respectively.

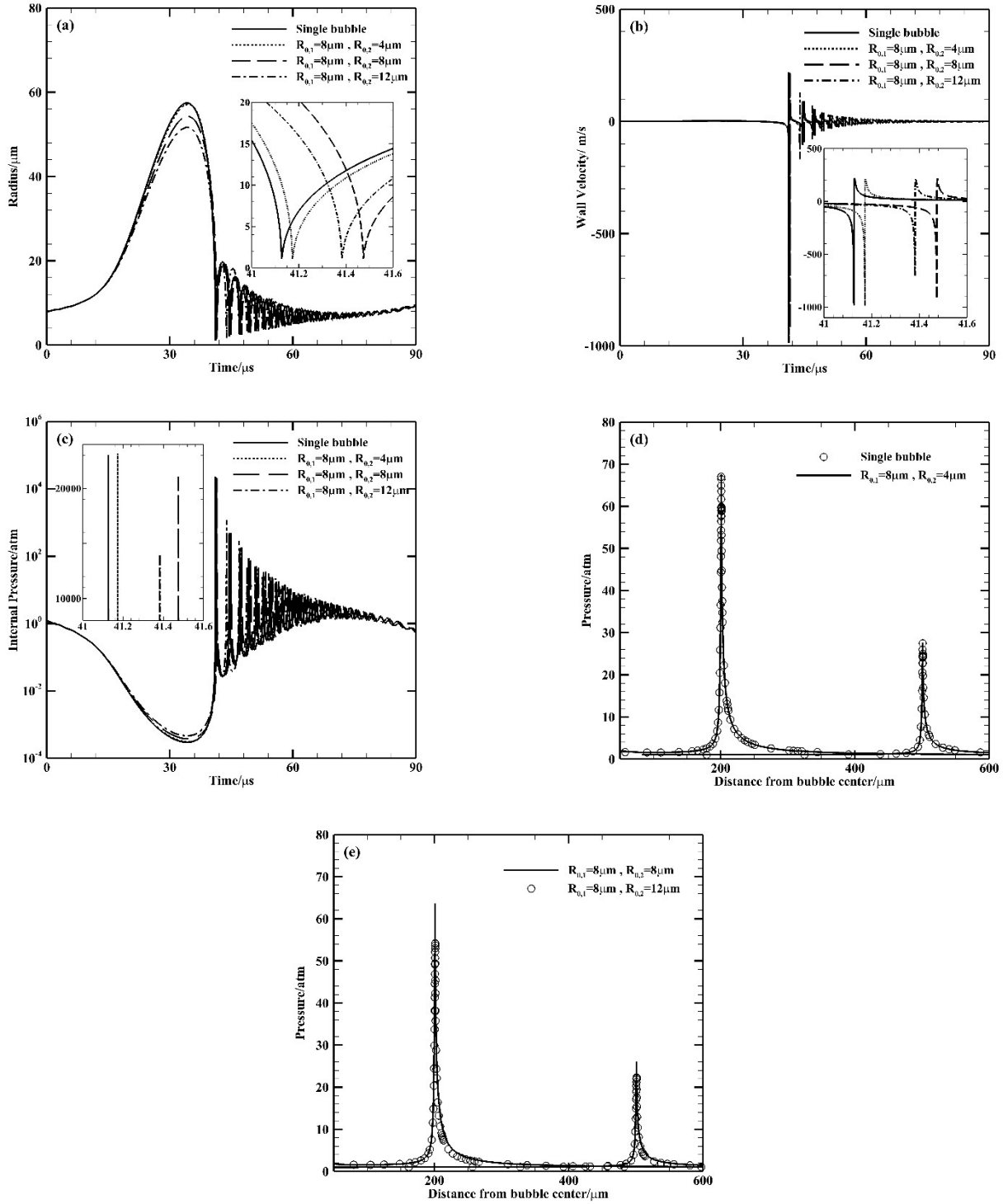

Fig. 4. Behavior of 8-μm bubble in single-bubble mode and in the presence of other bubbles at D = 200 μm. (a) Bubble radius, (b) bubble wall velocity, (c) bubble internal pressure, (d) and (e) propagated pressure wave.

For a more clear understanding, the interaction term $I = 1/D\,(2R\dot{R}^2 + R^2\ddot{R})$ which describes the bubble-bubble interaction in Eq. (9) is discussed more precisely. This term is plotted in Fig. 5(a-c) at the collapse moment of the 8-μm bubble and the index j in this term is related to the bubbles with the initial radii of R_0 =4 μm, R_0 =8 μm, and R_0 =12 μm. For a better comparison, the magnitudes of this term are also plotted for the 8-μm bubble at the collapse moment of other bubbles. As can

be seen, within the period of 41-42 μs, the amount of the interaction term for the 8-μm bubble is significantly increased in all three cases. However, the interaction of 4-μm and 12-μm bubbles shows a sharp decrease in the cases (a) and (c). The reason for the increase in the amount of the interaction term is the propagation of shock wave after the 8-μm bubble collapse. The negative value of I reflects the return of this wave after colliding with 4-μm and 12-μm bubbles. Due to not considering the time required to proceed in Eq. (9), these negative values are depicted exactly at the collapse moment of the 8-μm bubble. The magnitude of the return wave is directly proportional to the instantaneous radius of the bubble and the intensity of the shock wave emitted from the other bubble and is inversely proportional to the distance between the bubbles [29]. As shown in Fig. 4(d,e), the shock wave propagated from the 8-μm bubble in the presence of 4-μm bubble is about 1.3 times of the shock strength propagated in the presence of the 12-μm bubble; while the radius of the 12-μm bubble at the collapse point of 8-μm bubble is about 14 times of the radius of the 4-μm bubble at the collapse point of 8-μm bubble (figures are not shown). In other words, the greater ratio of radii results in an increase in the negative value of I in part (a) compared to part (c) in Fig. 5.

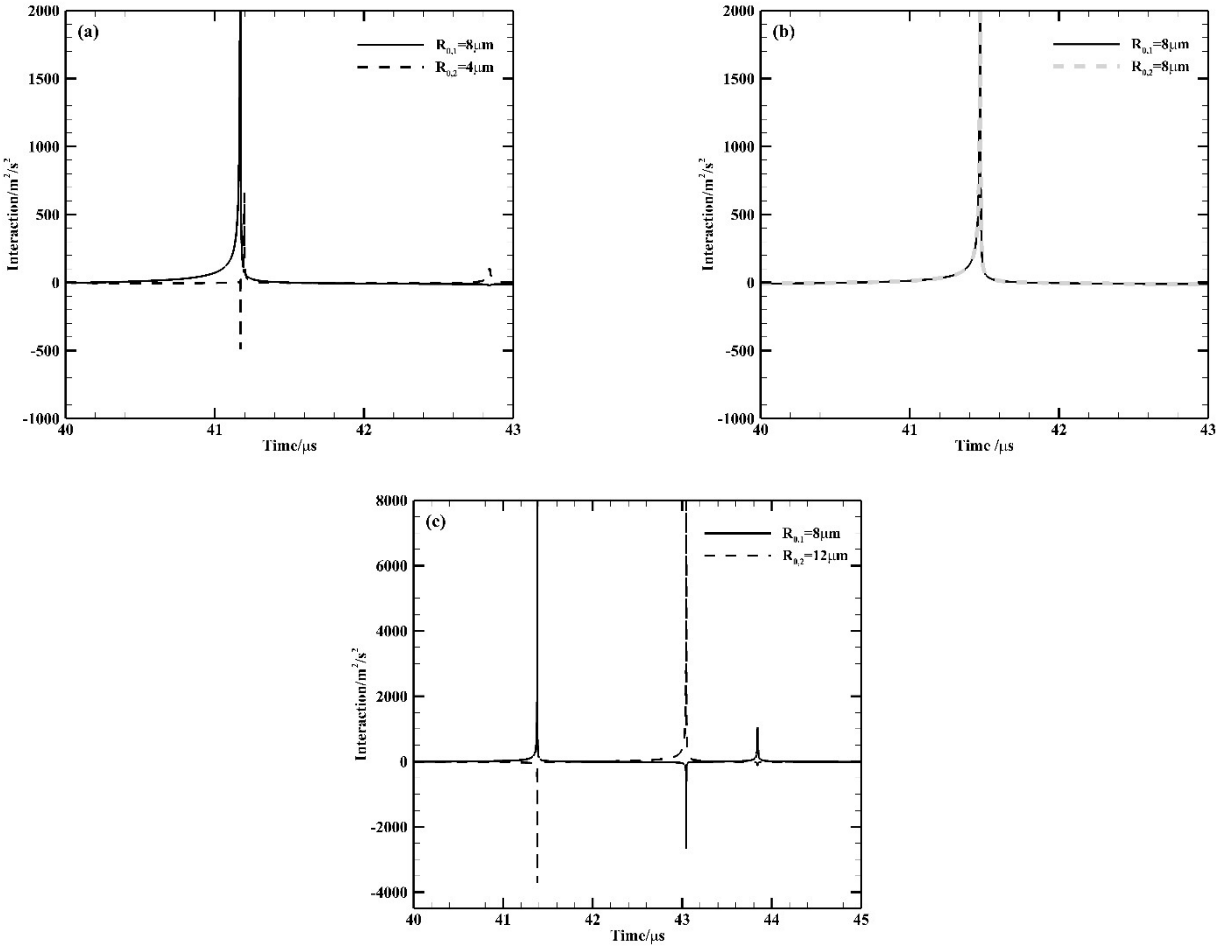

Fig. 5. Values of interaction term for three different oscillation modes when the distance between bubbles is 200 μm. (a) 8-4 μm mode (b) 8-8 μm mode (c) 8-12 μm mode

Another point is the absence of negative interaction value in Fig. 5b, in which two bubbles have the same radius and oscillate synchronically. In this case, at the moment of shock wave propagation, both bubbles are in their most compressed state and their internal pressure is the highest. Therefore, the pressure wave of a bubble does not have enough power to compress the other bubble. As a result, the negative values are not formed and only positive values of I are plotted on the graph.

3.2.2. Effect of bubbles central distance

To investigate the distance effect, the comparison is made between the behavior of the 8-μm bubble in the presence of other bubbles at 500 μm and 200 μm distances. Since the distance effect depends on the radius of the bubbles, the focus is initially on the 8-μm bubble next to the 12-μm bubble as a smaller bubble, and then on the 8-μm bubble adjacent to the 4-μm bubble as a larger one.

Figure 6 shows the behavior of the bubble with the initial size of R_0 = 8 μm when the 12-μm bubble is located at distances of 200 μm and 500 μm from its center. It can be seen in Fig. 6(a) that as the gap between the bubbles increases, the effect of the larger bubble on the smaller bubble decreases and the smaller bubble radius grows by about 6 percent. As shown in Fig. 6(b), increasing the distance between centers rises the wall velocity more than 20 percent. In Figs. 6(c) and 6(d), the increase in the distance between the bubbles also rises the maximum internal pressure about 38 percent and the shock wave power about 13 percent, respectively. In other words, by increasing the distance between bubbles, the effect of bubbles on each other decreases and their behavior becomes closer to the single-bubble state.

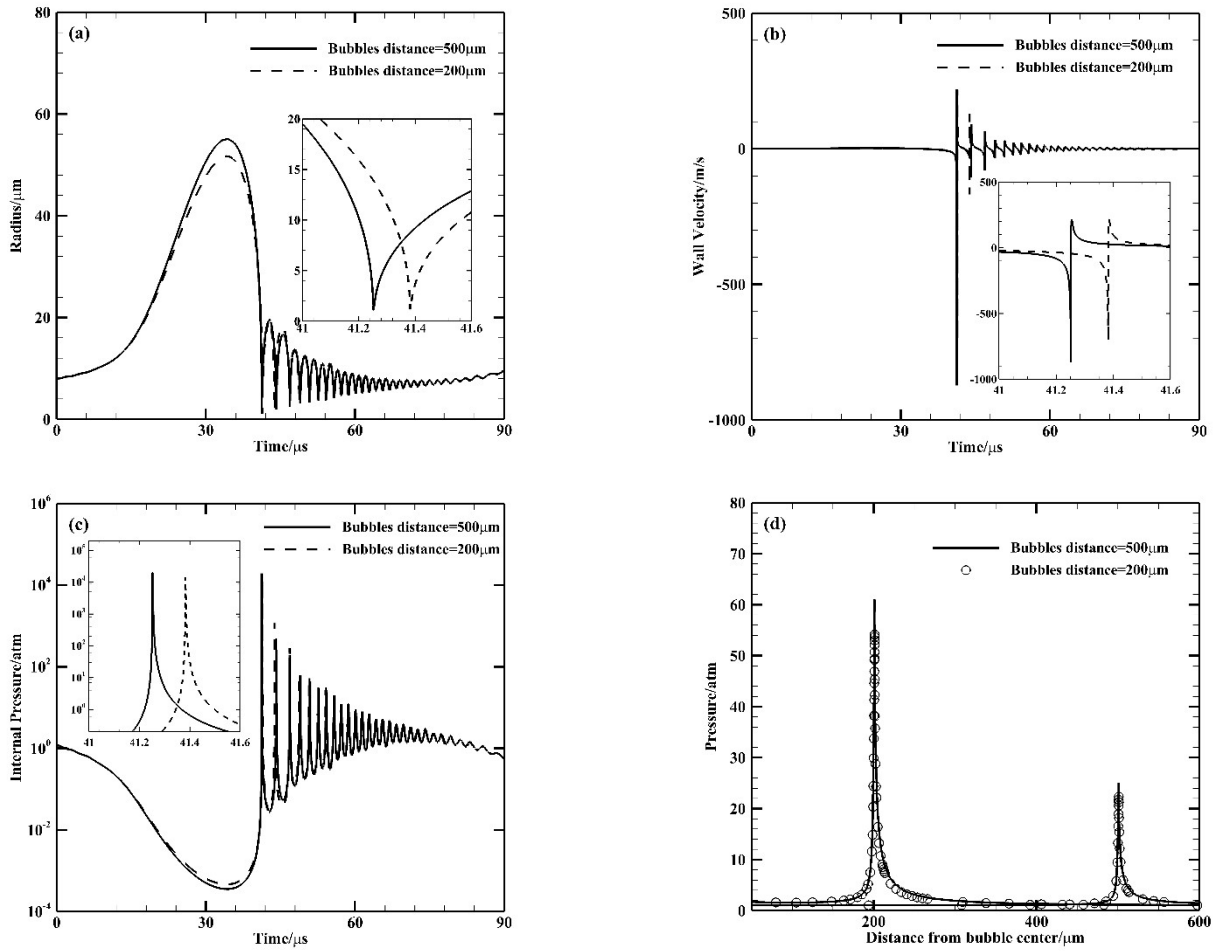

Fig. 6. Behavior of 8-μm bubble in single-bubble mode and in the presence of 12-μm bubble at different distances. (a) Bubble radius, (b) bubble wall velocity, (c) bubble internal pressure, and (d) propagated pressure wave.

In order to investigate the effect of distance on the larger bubble, the behavior of the 8-μm bubble is shown in the presence of the 4-μm bubble. Figure 7(a-d) indicates variations of the radius, the wall velocity, the internal pressure, and the shock wave, respectively. As is shown, the values of these terms remained almost unchanged for D = 200 μm and D = 500 μm. In other words, unlike the previous state, the effect of the distance change on the larger bubble is very low so that the behavior of the larger bubble can be considered independent of its distance from the smaller one.

In Figure 8, the value of I is shown for 8-12 and 8-4 situations when the distance between bubbles is 500 μm. In this case, as already mentioned, the main reason for the difference between the first negative values of I in parts *a* and *b* is the difference between the instantaneous radii of 12-μm and 4-μm bubbles at the collapse point of the 8-μm bubble. The reason for the overall reduction of these values in comparison with Fig. 5 is the absorption of the shock wave power by the fluid over the time and the increase in the distance between bubbles.

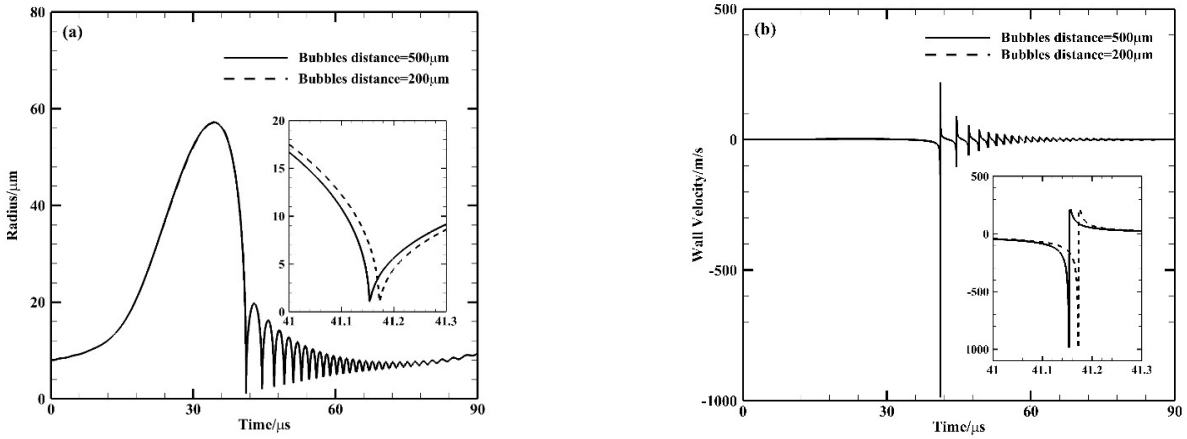

Fig. 7. The behavior of 8-μm bubble in single-bubble mode and in the presence of 4-μm bubble at different distances. (a) Bubble radius, (b) bubble wall velocity, (c) bubble internal pressure, and (d) propagated pressure wave.

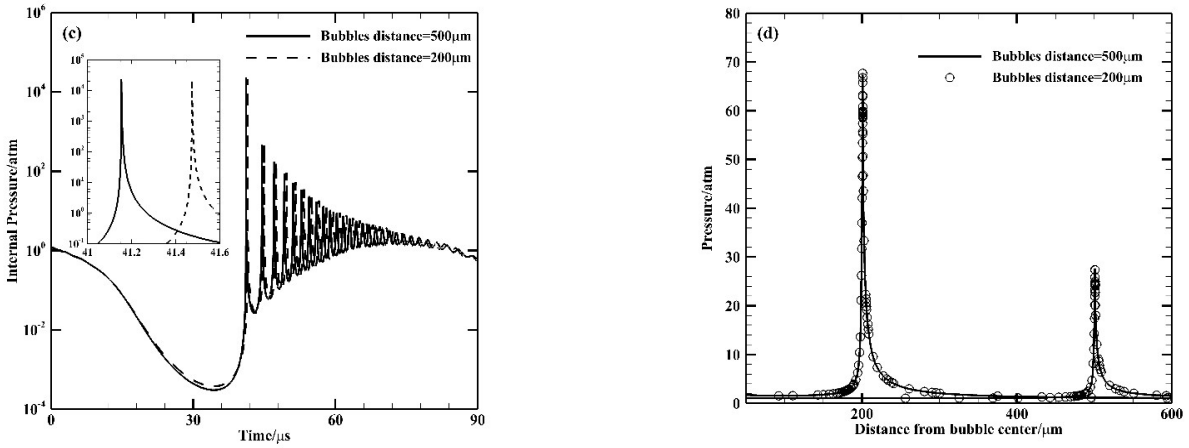

Fig. 7. Continued

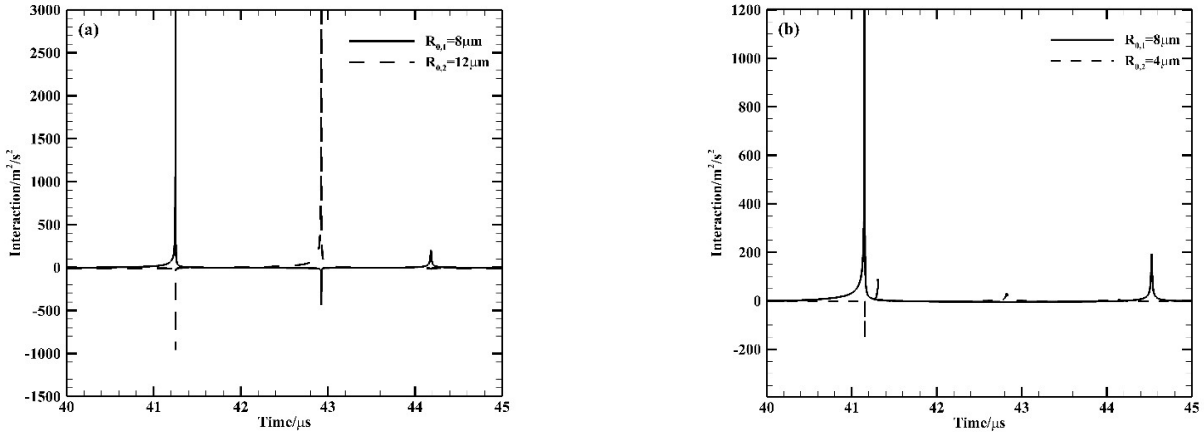

Fig. 8. Magnitude of interaction term for bubble with initial radius of 8-μm in the presence of (a) 12-μm and (b) 4-μm bubbles in 500 μm distance

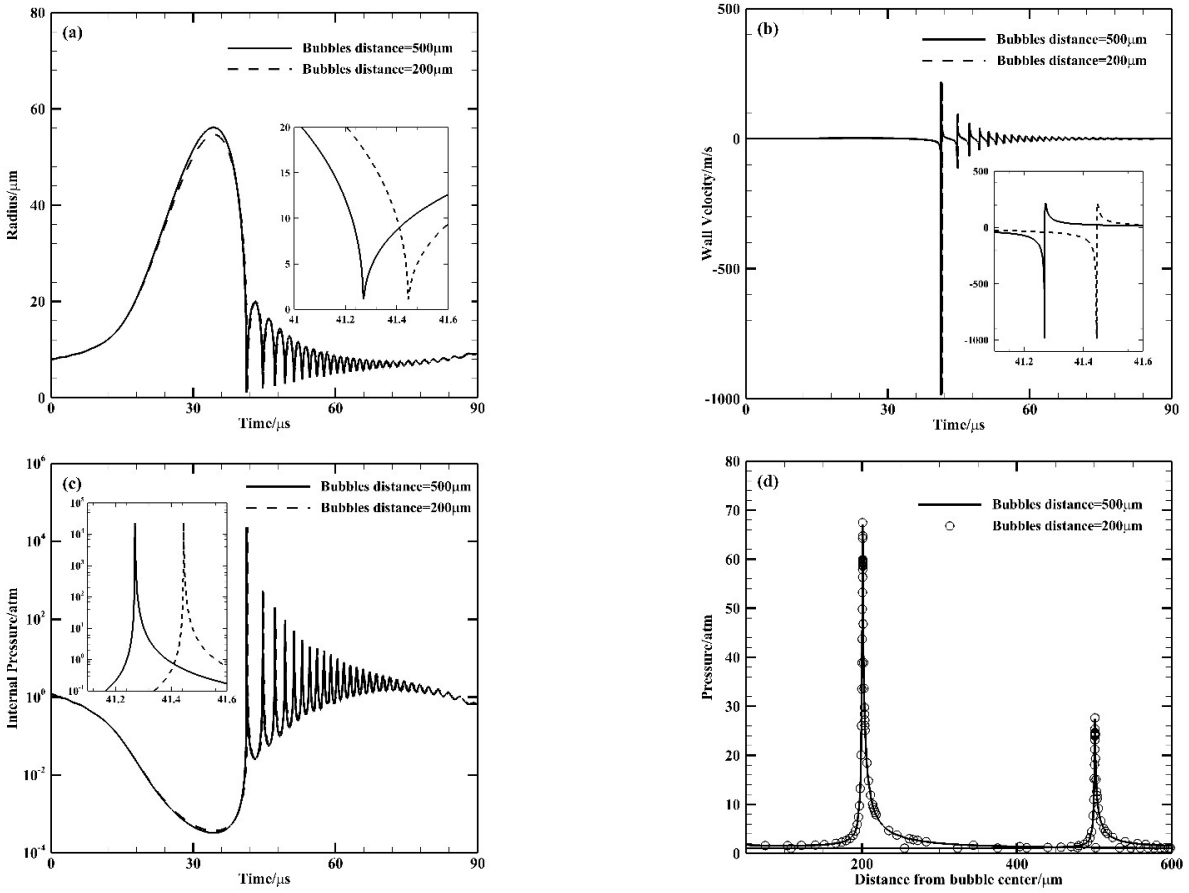

Fig. 9. The behavior of 8-μm bubble in single-bubble mode and in the presence of 7.5-μm bubble at different distances. (a) Bubble radius, (b) bubble wall velocity, (c) bubble internal pressure, and (d) propagated pressure wave

So far, it is seen that changing the gap between two bubbles has an effect on the behavior of the smaller bubble, while it does not affect the larger one. Here the question arises that if the difference in radii of bubbles are low, does the distance still not affect the larger bubble? To answer this question, this time, the bubble behavior with the initial radius of R_0 =8 μm is investigated in the presence of the 7.5-μm bubble at 200 μm and 500 μm distances. As shown in Fig. 9, although reduction in the difference between the initial radii has a slight effect on the 8-μm bubble radius, there is still no change in the wall velocity, the internal pressure, and the shock wave diagrams. In other words, it can be said that even in cases with a small radius difference, the bubbles distance still has no significant impact on the behavior of the larger bubble.

4. Conclusion

In the present study, the mutual interaction of bubbles in an acoustic field and its effect on the strength of emitted pressure waves are numerically investigated. The modified Keller-Miksis equation is used to simulate the oscillatory motion of bubbles and the Gilmore equation is used to simulate the pressure waves released from the bubbles collapse. The effects of viscosity and compressibility are considered and it is assumed that bubbles maintain their spherical shape. The distribution of the pressure inside bubbles is assumed to be uniform and air and water are used as the gases inside bubbles and as the liquid in vicinity of bubbles, respectively. Delay effects, vapor pressure and mass exchanges are neglected and processes are considered to be adiabatic.

The results show that the interaction of bubbles significantly affects the dynamic behavior of the bubbles. In general, it can be said that the dynamic behavior of the smaller bubble is more affected by the neighboring bigger bubble. Numerical simulations reveal that the initial radii of bubbles play an important role in their mutual behavior so that as initial radius of the second bubble grows, it causes further reduction in the maximum values of radius, wall velocity, internal pressure and shock wave strength of the first bubble. Moreover, the theoretical analysis indicates that there is a lag in the oscillation of the bubbles in the multi-bubble case in comparison with the single-bubble case. This lag is due to the existence of interaction term in the bubbles oscillation equation.

It is also found that the bubbles center-to-center distance is another important factor which changes the strength of the coupling effect. In this case, if the bubble is placed in the vicinity of the larger bubble, increasing the bubbles distance causes the growth of the radius, wall velocity, internal pressure, and shock wave strength of the smaller bubble. On the other hand, if the bubble is located in the vicinity of the smaller bubble, increasing the distance does not significantly affect the behavior of the larger bubble. In the case where the difference between the initial radius of the bubbles is small, although increasing the gap between bubbles causes a slight change in the maximum radius of the larger bubble, there is still no change in the values of wall velocity, internal pressure, and shock strength of the larger bubble. Therefore, it can be said that in this case the behavior of the larger bubble is independent of its distance from the smaller one.

Conflict of Interest

The authors declare no conflict of interest.

References

[1] C. Cogné, S. Labouret, R. Peczalski, O. Louisnard, F. Baillon, F. Espitalier, Theoretical model of ice nucleation induced by acoustic cavitation. Part 1: Pressure and temperature profiles around a single bubble, *Ultrason. Sonochem.* 29 (2016) 447–454.
[2] K.R. Weninger, B.P. Barber, S.J. Putterman, Pulsed Mie scattering measurements of the collapse of a sonoluminescing bubble, *Phys. Rev. Lett.* 78 (1997) 1799.
[3] M.P. Brenner, S. Hilgenfeldt, D. Lohse, Single-bubble sonoluminescence, *Rev. Mod. Phys.* 74 (2002) 425.
[4] C. Cairós, R. Mettin, Simultaneous High-Speed Recording of Sonoluminescence and Bubble Dynamics in Multibubble Fields, *Phys. Rev. Lett.* 118 (2017) 64301.
[5] L.A. Crum, R.A. Roy, Sonoluminescence, *Phys. Today.* 47 (1994) 22–30.
[6] H.-Y. Kwak, H. Yang, An aspect of sonoluminescence from hydrodynamic theory, *J. Phys. Soc. Japan.* 64 (1995) 1980–1992.
[7] K.S. Suslick, N.C. Eddingsaas, D.J. Flannigan, S.D. Hopkins, H. Xu, Extreme conditions during multibubble cavitation: Sonoluminescence as a spectroscopic probe, *Ultrason. Sonochem.* 18 (2011) 842–846.
[8] A. Shima, Studies on bubble dynamics, *Shock Waves* 7 (1997) 33–42.
[9] A. Philipp, W. Lauterborn, Cavitation erosion by single laser-produced bubbles, *J. Fluid Mech.* 361 (1998) 75–116.
[10] N.K. Bourne, On the collapse of cavities, *Shock Waves* 11 (2002) 447–455.
[11] C.D. Ohl, Cavitation inception following shock wave passage, *Phys. Fluids.* 14 (2002) 3512–3521.
[12] L.A. Crum, Bjerknes forces on bubbles in a stationary sound field, *J. Acoust. Soc. Am.* 57 (1975) 1363–1370.
[13] M. Ida, Alternative interpretation of the sign reversal of secondary Bjerknes force acting between two pulsating gas bubbles, *Phys. Rev. E.* 67 (2003) 56617.
[14] R. Mettin, I. Akhatov, U. Parlitz, C. Ohl, W. Lauterborn, Bjerknes forces between small cavitation bubbles in a strong acoustic field, *Phys. Rev. E.* 56 (1997) 2924–2931.
[15] N. Rezaee, R. Sadighi-Bonabi, M. Mirheydari, H. Ebrahimi, Investigation of a mutual interaction force at different pressure amplitudes in sulfuric acid, *Chinese Phys. B.* 20 (2011) 87804.

[16] L.W. Chew, E. Klaseboer, S.-W.W. Ohl, B.C. Khoo, Interaction of two differently sized oscillating bubbles in a free field, *Phys. Rev. E - Stat. Nonlinear, Soft Matter Phys.* 84 (2011) 66307.
[17] W. Lauterborn, C. Ohl, The Peculiar Dynamics of Cavitation Bubbles, *Appl. Sci. Res.* 58 (1998) 63–76.
[18] P. Testud-Giovanneschi, A.P. Alloncle, D. Dufresne, Collective effects of cavitation: Experimental study of bubble-bubble and bubble-shock wave interactions, *J. Appl. Phys.* 67 (1990) 3560–3564.
[19] K.S. Suslick, D.A. Hammerton, R.E. Cline, Sonochemical hot spot, *J. Am. Chem. Soc.* 108 (1986) 5641–5642.
[20] Lord Rayleigh, VIII. On the pressure developed in a liquid during the collapse of a spherical cavity, *Philos. Mag. Ser.* 6(34) (1917) 94–98.
[21] F.R. Gilmore, The growth or collapse of a spherical bubble in a viscous compressible liquid, Hydrodyn. Lab. Calif. Inst. Technol. Pasadena, Calif. Report, 26 (1952) 41.
[22] J.B. Keller, M. Miksis, Bubble oscillations of large amplitude, *J. Acoust. Soc. Am.* 68 (1980) 628–633.
[23] M.S. Plesset, The dynamics of cavitation bubbles, *J. Appl. Mech.* 16 (1949) 277–282.
[24] D. Fuster, C. Dopazo, G. Hauke, Liquid compressibility effects during the collapse of a single cavitating bubble, *J. Acoust. Soc. Am.* 129 (2011) 122–131.
[25] V. Minsier, J. Proost, Shock wave emission upon spherical bubble collapse during cavitation-induced megasonic surface cleaning, *Ultrason. Sonochem.* 15 (2008) 598–604.
[26] M. Mahdi, M. Shams, R. Ebrahimi, Effects of heat transfer on the strength of shock waves emitted upon spherical bubble collapse, *Int. J. Numer. Methods Heat Fluid Flow* 20 (2010) 372–391.
[27] S.J. Shaw, P.D.M. Spelt, D.L. Higher, Shock emission from collapsing gas bubbles, *J. Fluid Mech.* 646 (2010) 363.
[28] S.W. Karng, Y.P. Lee, K.Y. Kim, H.Y. Kwak, Implosion mechanism for a sonoluminescing gas bubble, *J. Korean Phys. Soc.* 43 (2003) 135–144.
[29] M. Ida, Bubble-bubble interaction: A potential source of cavitation noise, *Phys. Rev. E.* 79 (2009) 16307.
[30] R. Sadighi-Bonabi, N. Rezaee, H. Ebrahimi, M. Mirheydari, Interaction of two oscillating sonoluminescence bubbles in sulfuric acid, *Phys. Rev. E.* 82 (2010) 1–7.
[31] F. Li, J. Cai, X. Huai, B. Liu, Interaction mechanism of double bubbles in hydrodynamic cavitation, *J. Therm. Sci.* 22 (2013) 242–249.
[32] D.J. Flannigan, S.D. Hopkins, C.G. Camara, S.J. Putterman, K.S. Suslick, Measurement of pressure and density inside a single sonoluminescing bubble, *Phys. Rev. Lett.* 96 (2006) 204301.